Tree demographics and soil charcoal evidence of fire disturbances in an inaccessible forest atop the Mount Lico inselberg, Mozambique

Courtney Mustaphi, Colin; Platts, Philip J.; Willcock, Simon; Timberlake, Jonathan; Osborne, Jo; Matimele, Hermenegildo; Osgood, Hanniah; Muiruri, Veronica; Gehrels, Maria; Bayliss, Julian; Marchant, Robert

Plants, People, Planet

Accepted/In press: 03/09/2024

Peer reviewed version

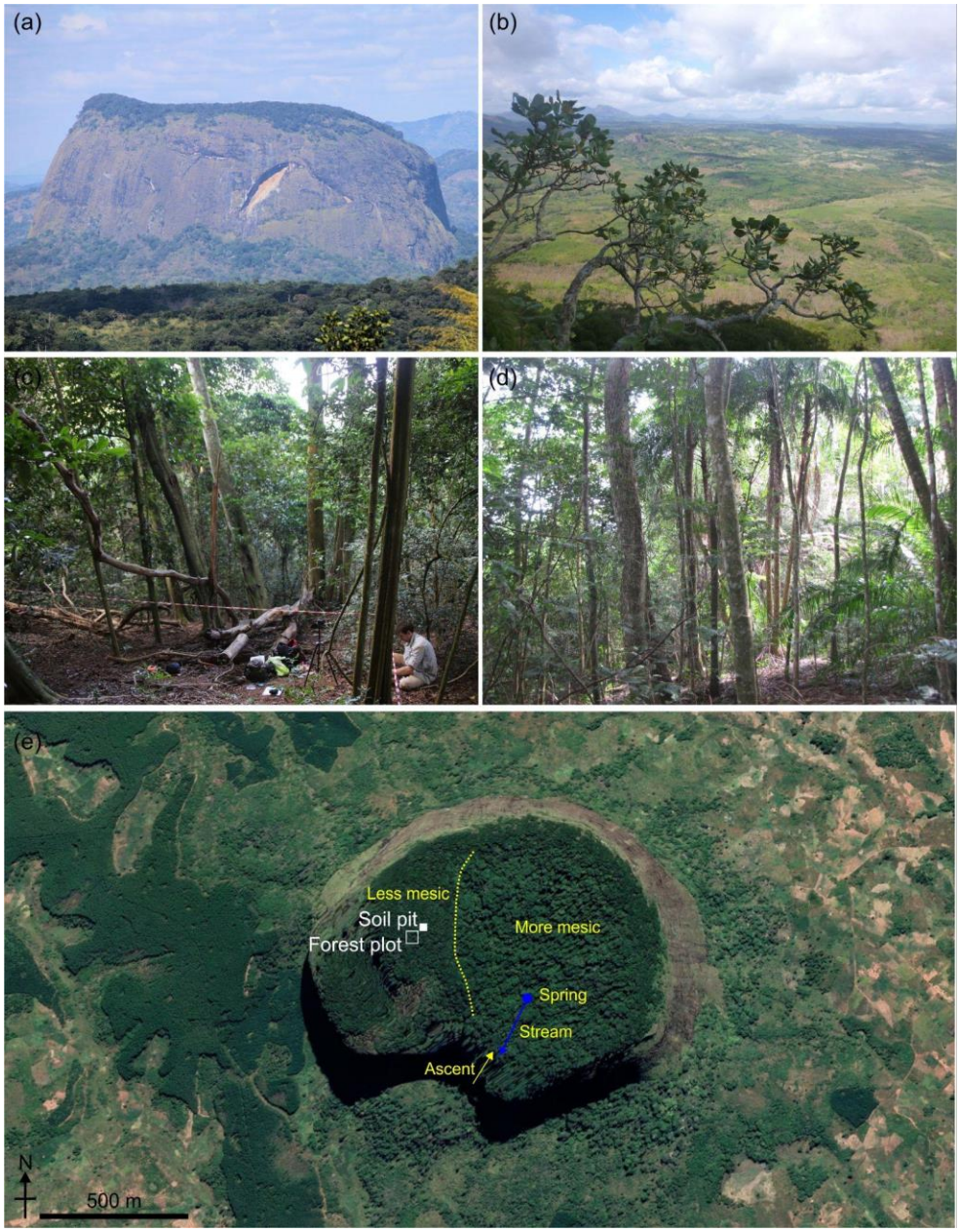

FIGURE 1 Photographs of (a) Mount Lico, Mozambique, located at geographic coordinates 15.792 °S, 37.363 °E, and (b) a view of the surrounding landscape from Mount Lico. Both (c) and (d) show examples of evergreen and semi-deciduous forest on top of Mount Lico. (e) Satellite-based view of Mount Lico and surrounding patches of agricultural and forested landscape showing the study site soil pit location (solid white square), 20x20 m forest plot (open white square) and the apparent east-west moisture gradient and approximate ecotone between forest types. Photographs (a–c), Phil Platts, and (d), Simon Willcock, May-June 2018. Satellite image dated May 2021 accessed through Google Earth Pro version 7.3.4.8642 (64-bit) with 2.0× vertical exaggeration to show topographic relief (Google LLC/Maxar Technologies, 2022).

FIGURE 2 Photographs of the (a) 2.2 m deep soil pit profile on Mount Lico, and (b–c) subsample collection down the soil profile. Photographs (a), Phil Platts, and (b–c), Simon Willcock, May 2018.

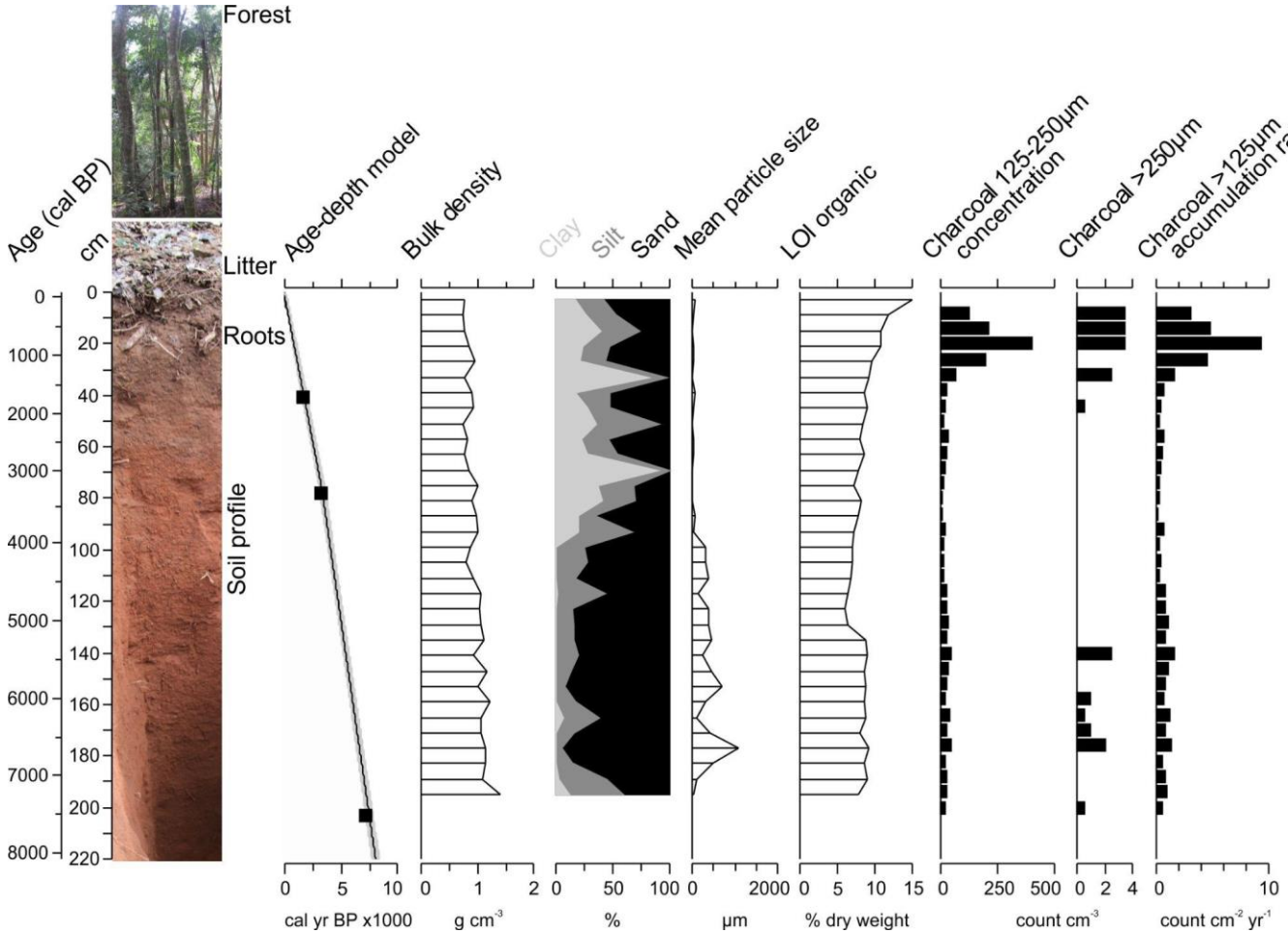

FIGURE 3 Summary results of the 220 cm soil profile. Note the limited O layer and relatively weak differentiation of the A and B horizon colouration at 50 cm. Radiocarbon age determinations and a linear interpolation age-depth model of the calibrated radiocarbon ages (black squares, n=3, see Supplemental Table 1; SHCal20; Hogg et al., 2020). Soil density and textural measurements and loss-on-ignition organic content estimated. Sieved soil charcoal results that show concentration and accumulation rate values.

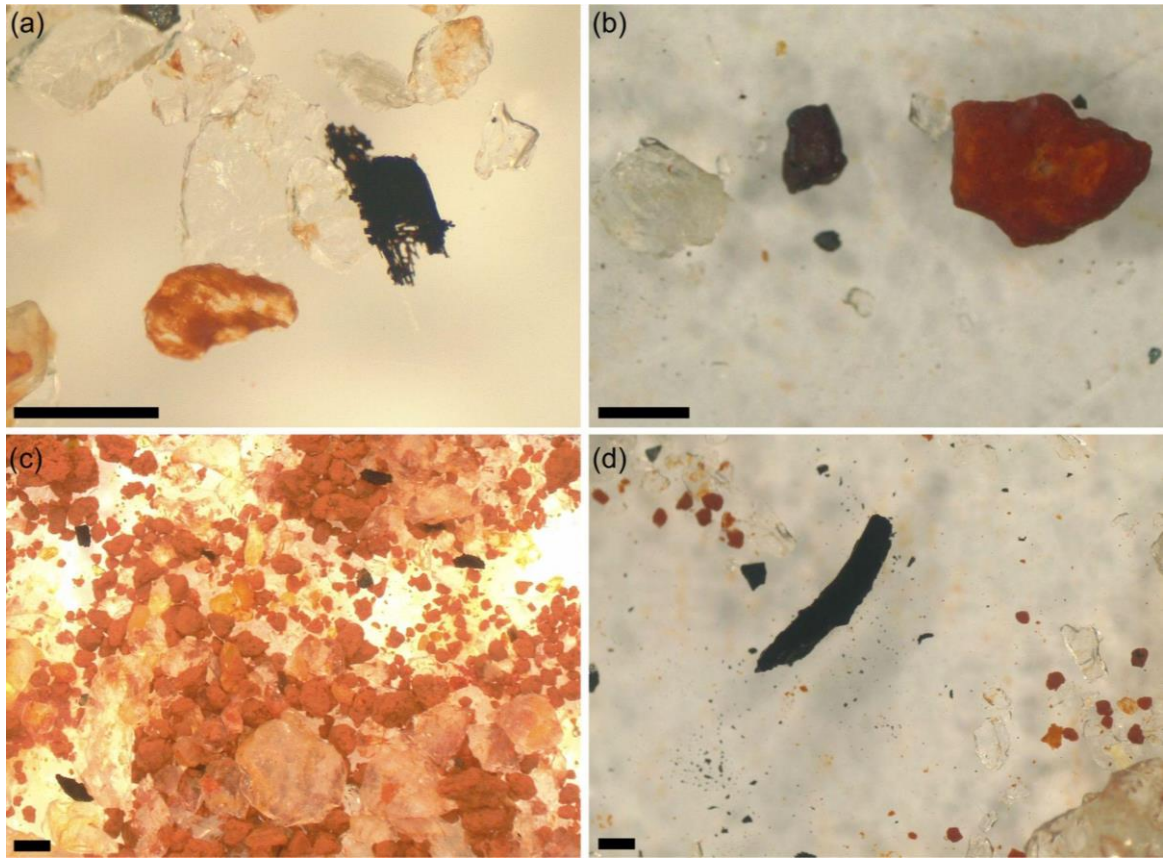

FIGURE 4 Digital photographs of wet sieved subsamples. (a) Herbaceous charcoal, imperfect fragmented morphotype B5, at 20–22 cm depth (809–896 cal BP). (b) The three most abundant very coarse silt and sand grains throughout the core, quartz, magnetite, and reddish cemented clastic aggregates, at 50–52 cm depth (2133–2222 cal BP). (c) Sand grains and charcoal fragments photographed at low power magnification (5x) from 140–142 cm depth (5421–5487 cal BP). (d) Larger 3-dimensional blocky and long charcoal (morphotype E, 3-dimensionality is less apparent in photograph) fragment of non-woody plant part, highly resistant to entrainment, at 176–178 cm depth (6615–6681 cal BP). Black scale bar represents 200 μm.

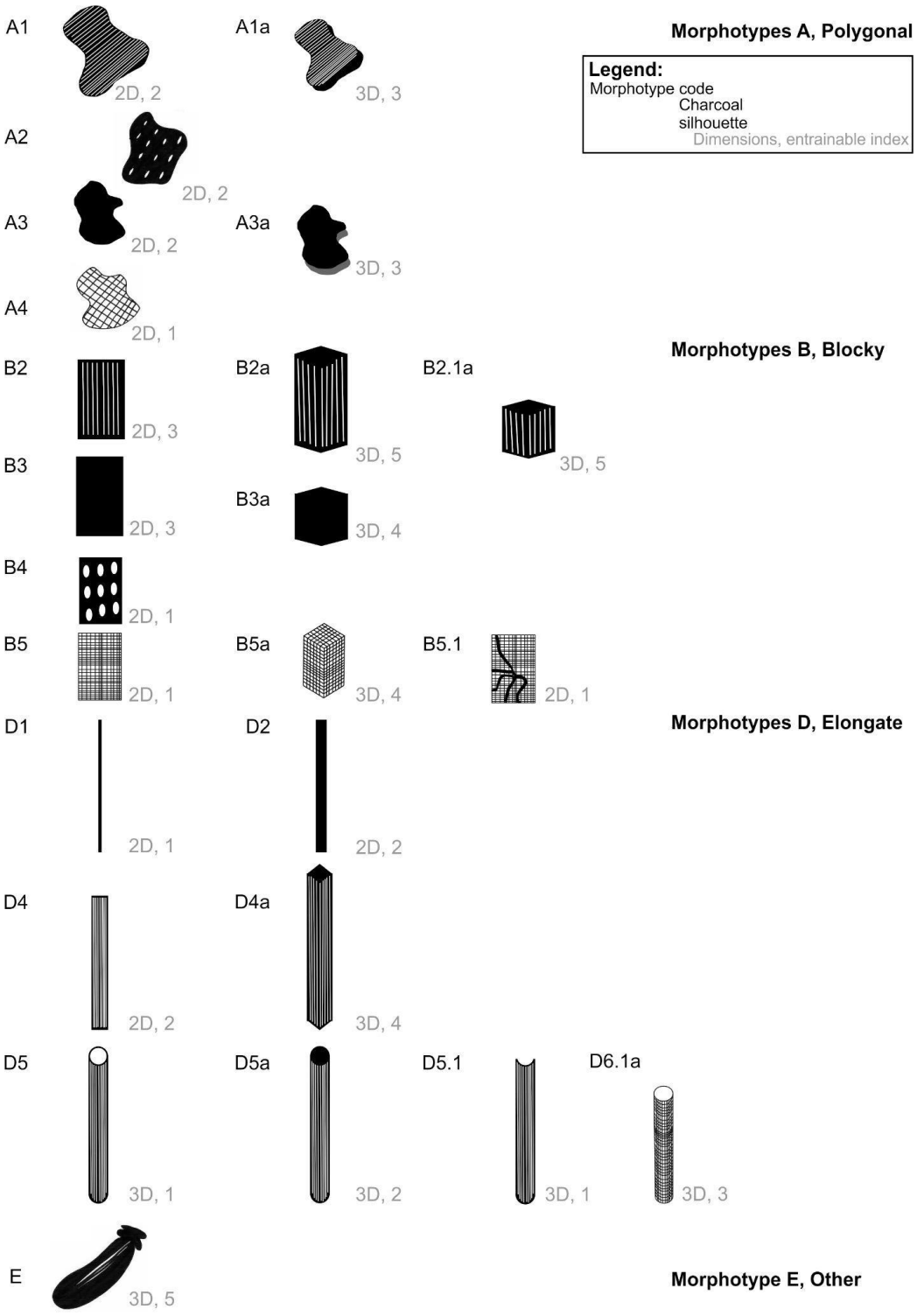

FIGURE 5 Idealised charcoal morphotypes found in the Mount Lico soil pit profile (>125 μm). Charcoal fragment dimensionality apparent at 10–40x magnification observational scales (2 or 3 dimensional) and qualitative entrainable index value designated for each morphotype are shown in grey text (Table S2 and Figures 6 and 7). Solid black top faces on 3-dimensional charcoal represent solid internal, white top faces represent an open internal 3-dimensional morphotype.

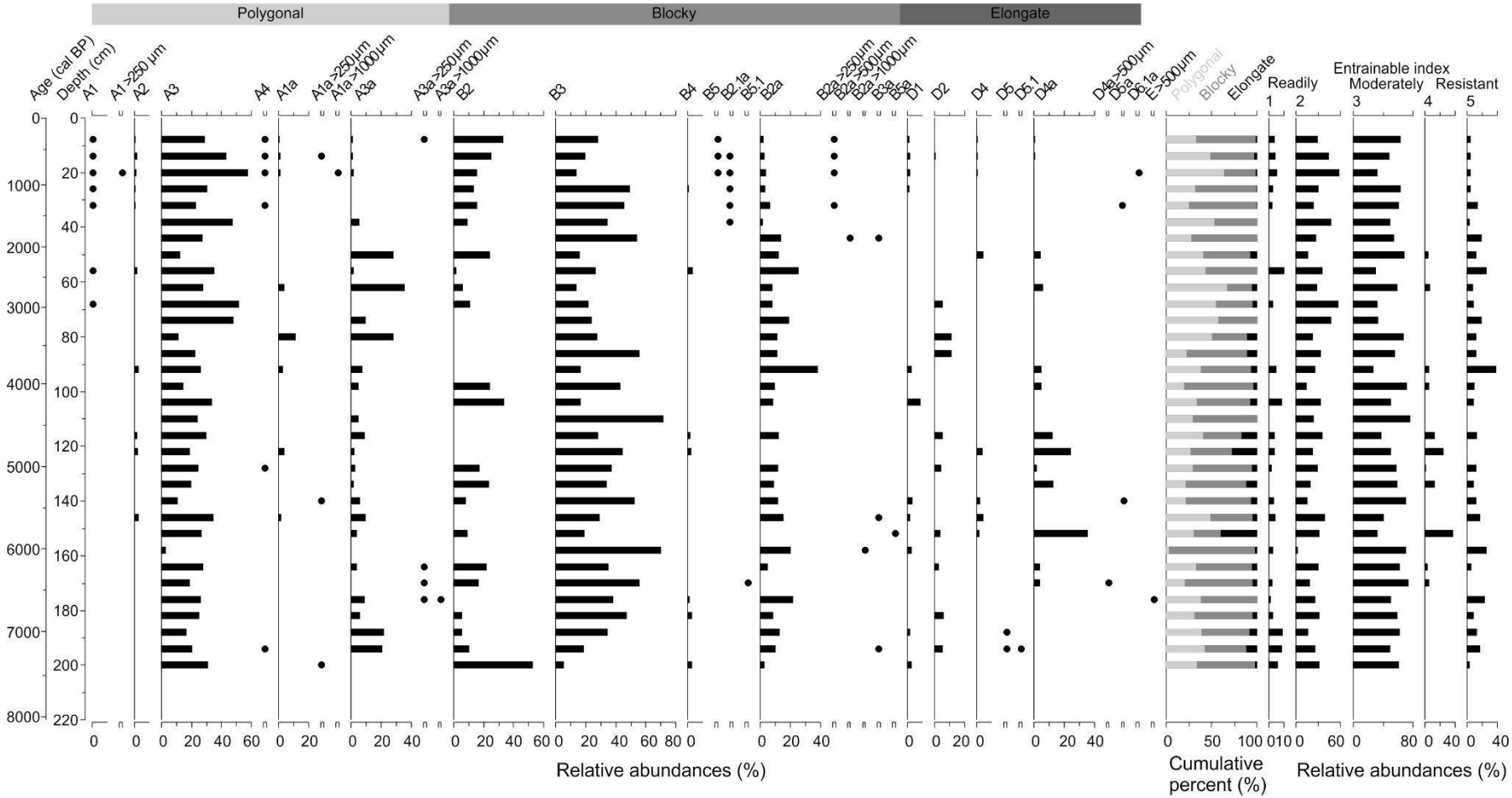

FIGURE 6 Charcoal morphology assemblage (>125 µm). A1 to D6 morphotype classifications and a single other type (morphotype E) (Figure 5). Cumulative total morphotype classes, Polygonal (Type A), Blocky (Type B) and Elongate (Type D) charcoal. Entrainable index 1 = easily entrainable and transported by air or water, and 5, resistant to transport entrainment and tends to remain locally deposited scaled by relative abundance (Table S2).

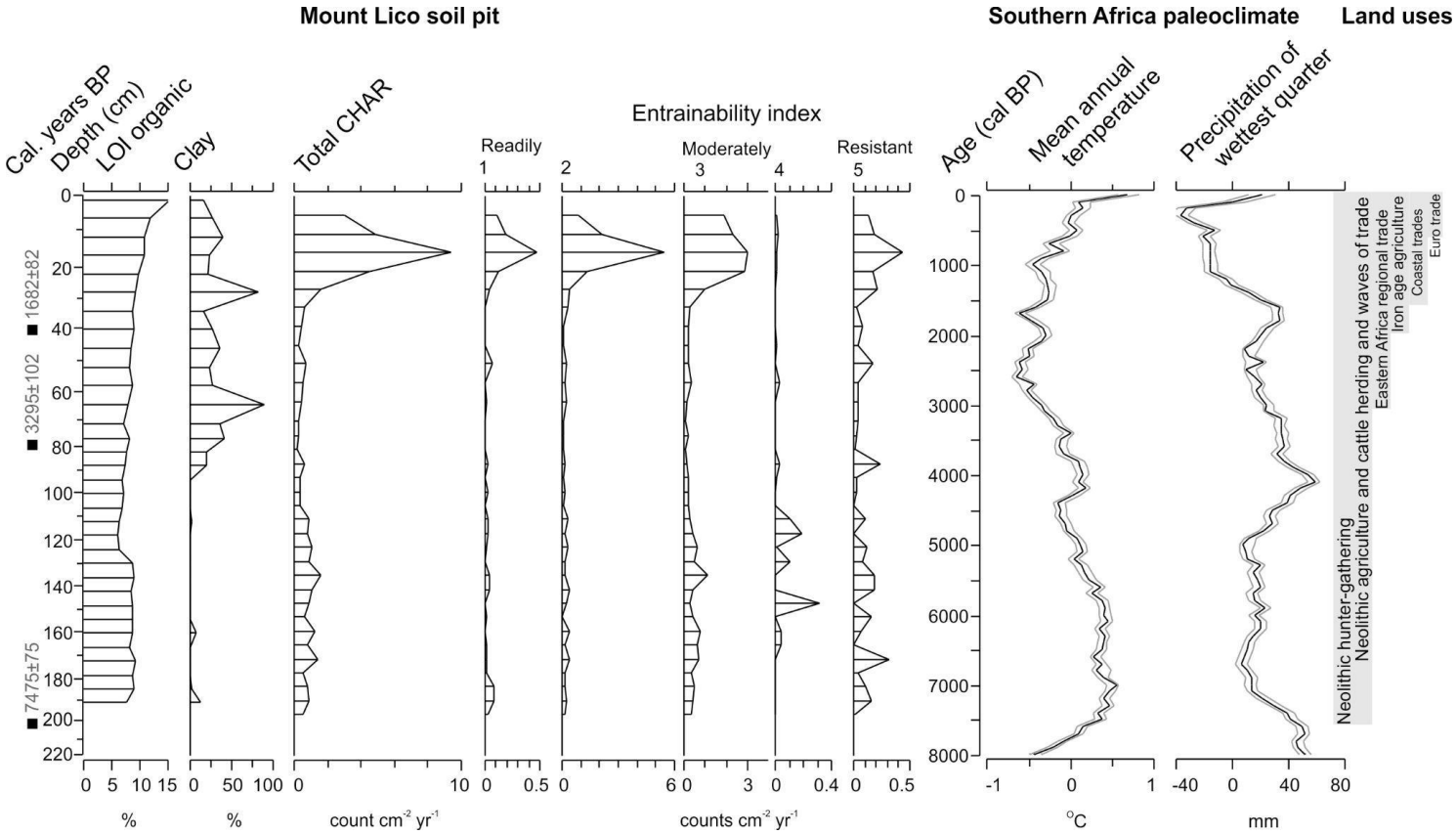

FIGURE 7 Select Mount Lico soil pit data (Figures 3, 5) and the accumulation rate of entrainable charcoal (sum of charcoal morphotype accumulation rates by each index value, 1–5; Figure 6). Paleoclimate reconstruction stacks of mean annual temperature anomaly reconstruction and precipitation of the wettest quarter of the year, binned to 100 year time steps (black lines) with 10% confidence envelope (grey lines) (Chase et al., 2017, paleoclimate product resolution of 100 year time steps). Generalised summary of past land use changes in eastern Africa (Morais, 1984; Nurse and Spear, 1985; Spear, 2000; Lane, 2004; Ekblom, 2012, 2018; Ekblom et al., 2011, 2014, 2016; Sinclair et al., 2014; Fleisher et al., 2015; Marchant et al., 2018; Ichumbaki and Pollard, 2021).